

Breaking the Madry Defense Model with L_1 -based Adversarial Examples

Yash Sharma¹ and Pin-Yu Chen²

¹The Cooper Union, New York, NY 10003, USA

²AI Foundations Group, IBM T. J. Watson Research Center, Yorktown Heights, NY 10598, USA
ysharma1126@gmail.com, pin-yu.chen@ibm.com

Abstract

The Madry Lab recently hosted a competition designed to test the robustness of their adversarially trained MNIST model. Attacks were constrained to perturb each pixel of the input image by a scaled maximal L_∞ distortion $\epsilon = 0.3$. This discourages the use of attacks which are not optimized on the L_∞ distortion metric. Our experimental results demonstrate that by using the **elastic-net attack** to **deep** neural networks (EAD), one can generate transferable adversarial examples which, despite their high average L_∞ distortion, have minimal visual distortion. These results call into question the use of L_∞ as a sole measure for visual distortion, and further demonstrate the power of EAD at generating robust adversarial examples.

1 Introduction

Deep neural networks (DNNs) achieve state-of-the-art performance in various tasks in machine learning and artificial intelligence, such as image classification, speech recognition, machine translation and game-playing. Despite their effectiveness, recent studies have illustrated the vulnerability of DNNs to adversarial examples [5, 7]. For instance, a carefully designed perturbation to an image can lead a well-trained DNN to misclassify. Even worse, effective adversarial examples can also be made virtually indistinguishable to human perception. Adversarial examples crafted to evade a specific model can even be used to mislead other models trained for the same task, exhibiting a property known as transferability.

To address this problem, the adversarial robustness of neural networks was studied through the lens of robust optimization by Madry et al. [4], leading to an adversarially robust model for image classification we term as the “Madry Defense Model”. An attack challenge¹ was proposed for the MNIST dataset to test the defense, however, attacks were constrained to perturb each pixel by at most $\epsilon = 0.3$, a scaled maximal L_∞ distortion. This rule greatly reduces the power of attacks which are not optimized for the L_∞ distortion metric, and imposes an unrealistic constraint on the attacker.

To justify the limitation of the L_∞ constraint, we conduct extensive experiments on the Madry Defense Model to investigate the transferability properties of the state-of-the-art adversarial attacks without the L_∞ constraint. We find that L_1 -based adversarial examples generated by EAD, which is short for **Elastic-net Attack to DNNs** [3], readily transfer in both the targeted and non-targeted cases, and despite the high L_∞ distortion, the visual distortion on the adversarial examples is minimal. These results call into question the use of L_∞ to quantify visual distortion, and further demonstrate the state-of-the-art transferability properties of EAD.

¹https://github.com/MadryLab/mnist_challenge

2 Experiment Setup

2.1 Madry Defense Model

In [4], the authors used a saddle point formulation to capture the notion of robustness against adversarial attacks in a principled manner. An experimental study was conducted regarding the optimization landscape corresponding to the saddle point formulation, and the findings provide evidence that first-order methods can reliably solve this problem. Furthermore, the authors motivate projected gradient descent (PGD) as a universal "first-order adversary" (see Section 2.2.2 for details), the strongest attack utilizing the local first-order information about the network.

In addition, the authors explored the impact of network architecture on adversarial robustness and found that model capacity plays an important role. They observe that to reliably withstand strong adversarial attacks, networks require a significantly larger capacity than for correctly classifying benign examples only. Therefore, the Madry Defense Model is a sufficiently high capacity network trained against the strongest possible adversary, which they deem to be Projected Gradient Descent (PGD) starting from random perturbations around the natural examples.

For the MNIST model, 40 iterations of PGD were run, with a step size of 0.01. Gradient steps were taken in the L_∞ norm. The network was trained and evaluated against perturbations of size $\epsilon = 0.3$. We experimentally show in the supplementary material that this is the maximum ϵ for which the Madry Defense Model can be successfully adversarially trained.

2.2 Attacks

We test the transferability properties of attacks in both the targeted case and non-targeted case on the adversarially trained Madry Defense Model. We test the ability for attacks to generate transferable adversarial examples using a single undefended model as well as an ensemble of undefended models, where the ensemble size was set to 3. We expect that if an adversarial example remains adversarial to multiple models, it is more likely to transfer to other unseen models [1]. We discuss results transferring from an ensemble in the following sections, and provide results transferring from a single undefended model in the supplementary material.

For generating adversarial examples, we compare the optimization-based approach and the fast gradient-based approach using EAD and PGD, respectively. The targeted attack formulations are discussed below, non-targeted attacks can be implemented in a similar fashion [3]. We denote by \mathbf{x}_0 and \mathbf{x} the original and adversarial examples, respectively, and denote by t the target class to attack.

2.2.1 EAD

EAD generalizes the state-of-the-art C&W L_2 attack [6] by performing elastic-net regularization, linearly combining the L_1 and L_2 penalty functions. The formulation is as follows:

$$\begin{aligned} & \text{minimize}_{\mathbf{x}} \quad c \cdot f(\mathbf{x}, t) + \beta \|\mathbf{x} - \mathbf{x}_0\|_1 + \|\mathbf{x} - \mathbf{x}_0\|_2^2 \\ & \text{subject to} \quad \mathbf{x} \in [0, 1]^p, \end{aligned} \tag{1}$$

where $f(x, t)$ is defined as:

$$f(\mathbf{x}, t) = \max\{\max_{j \neq t} [\mathbf{Logit}(\mathbf{x})]_j - [\mathbf{Logit}(\mathbf{x})]_t, -\kappa\}, \tag{2}$$

By tuning β , one trades off L_2 optimization with L_1 optimization. By tuning κ , one trades off minimizing the distortion with maximizing the confidence in the adversarial example. Therefore, increasing κ improves transferability but compromises visual quality.

We test EAD in both the general case and the special case where β is set to 0, which is equivalent to the C&W L_2 attack. We implement 9 binary search steps on the regularization parameter c (starting from 0.001) and run $I = 1000$ iterations for each step with the initial learning rate $\alpha_0 = 0.01$. For finding successful adversarial examples, we use the ADAM optimizer for the C&W attack and implement the projected FISTA algorithm with the square-root decaying learning rate for EAD [3].

Table 1: Comparison of tuned PGD, I-FGM, C&W, and EAD adversarial examples at various confidence levels. ASR means attack success rate (%). The distortion metrics are averaged over successful examples.

Attack Method	Confidence	Targeted				Non-Targeted			
		ASR	L_1	L_2	L_∞	ASR	L_1	L_2	L_∞
PGD	None	68.5	188.3	8.947	0.6	99.9	270.5	13.27	0.8
I-FGM	None	75.1	144.5	7.406	0.915	99.8	199.4	10.66	0.9
C&W	10	1.1	34.15	2.482	0.548	4.9	23.23	1.702	0.424
	30	69.4	68.14	4.864	0.871	71.3	51.04	3.698	0.756
	50	92.9	117.45	8.041	0.987	99.1	78.65	5.598	0.937
	70	34.8	169.7	10.88	0.994	99	119.4	8.097	0.99
EAD	10	27.4	25.79	3.209	0.876	39.9	19.19	2.636	0.8
	30	85.8	49.64	5.179	0.995	94.5	34.28	4.192	0.971
	50	98.5	93.46	7.711	1	99.6	57.68	5.839	0.999
	70	67.2	148.9	10.36	1	99.8	90.84	7.719	1

2.2.2 PGD

Fast gradient methods (FGM) use the gradient ∇J of the training loss J with respect to \mathbf{x}_0 for crafting adversarial examples [7]. For L_∞ attacks, which we will consider, \mathbf{x} is crafted by

$$\mathbf{x} = \mathbf{x}_0 - \epsilon \cdot \text{sign}(\nabla J(\mathbf{x}_0, t)), \quad (3)$$

where ϵ specifies the L_∞ distortion between \mathbf{x} and \mathbf{x}_0 , and $\text{sign}(\nabla J)$ takes the sign of the gradient.

Iterative fast gradient methods (I-FGM) were proposed in [8], which iteratively use FGM with a finer distortion, followed by an ϵ -ball clipping. We note that this is essentially projected gradient descent on the negative loss function.

In this paper, PGD was tested both with and without random starts. Consistent with the implementation in [4], 40 steps were used. As the classic I-FGM formulation does not include random starts, PGD without random starts shall be termed I-FGM for the remainder of the paper. For I-FGM, the step size was set to be $\epsilon/40$, which has been shown to be an effective attack setting in [2]. For PGD, the step size was set to be $2\epsilon/40$ in order to allow all pixels to reach all possible values.

3 Transferability Results

In our experiment, 1000 random samples from the MNIST test set were used. For the targeted case, a target class that is different from the original one was randomly selected for each input image. The results of the β tuning for EAD is provided in the supplementary material. It is observed that the highest attack success rate (ASR) in both the targeted and non-targeted cases was yielded at $\beta = 0.01$. This was in fact the largest β tested, indicating the importance of minimizing the L_1 distortion for generating transferable adversarial examples. Furthermore, as can be seen in the supplementary material, the improvement in ASR with increasing β is more significant at lower κ , indicating the importance of minimizing the L_1 distortion for generating transferable adversarial examples with minimal visual distortion. The results of the ϵ tuning for PGD and I-FGM are provided in the supplementary material. In the targeted case, the highest ASR was yielded at $\epsilon = 0.6$ and $\epsilon = 1$ for PGD and I-FGM, respectively. In the non-targeted case, at ϵ values greater than or equal to 0.8 and 0.9 for PGD and I-FGM, respectively, the highest ASR was yielded.

In Table 1, the results for tuning κ for C&W and EAD at $\beta = 0.01$ are provided, and are presented with the results for PGD and I-FGM at the aforementioned ϵ values for comparison. It is observed that in the targeted case, EAD outperforms C&W at all κ , and at the optimal $\kappa = 50$, EAD’s adversarial examples surprisingly have lower average L_2 distortion. We also find that both EAD and C&W at properly tuned κ outperform PGD and I-FGM with much lower L_1 and L_2 distortion.

In the non-targeted case, it is also observed that EAD outperforms C&W at all κ . However, it appears that PGD and I-FGM are superior or at least equivalent in power to EAD, as similar ASR is yielded at lower L_∞ distortion. We argue that the drastic increase in induced L_1 and L_2 distortion to generate said adversarial examples indicates greater visual distortion, and thus that the generated examples are less adversarial in nature. We examine this in the following section.

4 Visual Comparison

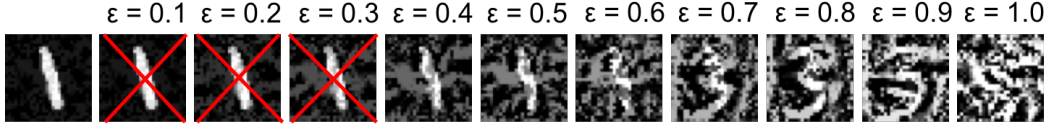


Figure 1: Visual illustration of adversarial examples crafted by PGD with ϵ tuned from 0.1 to 1.0 at 0.1 increments. The leftmost image is the original example. With $\epsilon \leq 0.3$, the adversarial examples were unsuccessful at transferring to the Madry Defense Model.

Adversarial examples generated by EAD and PGD were analyzed in the non-targeted case, to understand if the successful examples are visually adversarial. A similar analysis in the targeted case is provided in the supplementary material. In Figure 1, a selected instance (a hand-written ‘1’) of adversarial examples crafted by PGD at ϵ tuned from 0.1 to 1.0 at 0.1 increments is shown. As PGD simply operates on a L_∞ distortion budget, as ϵ increases, the amount of noise induced to all of the pixels in the image increases. This noise is visually obvious even at low ϵ such as 0.3, where the adversarial example does not even successfully transfer. At higher ϵ values, PGD appears to change the ‘1’ to a ‘3’. However, under such large visual distortion, it is not entirely clear.

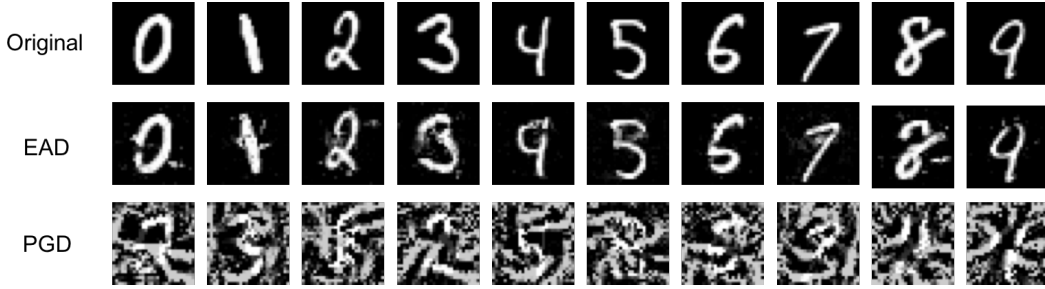


Figure 2: Visual illustration of adversarial examples crafted in the non-targeted case by EAD and PGD with similar average L_∞ distortion. Clearly, performing elastic-net minimization enables the generation of transferable images with minimal visual distortion.

In Figure 2, adversarial examples generated by EAD are directly compared to those generated by PGD with similar average L_∞ distortion. EAD tuned to the optimal β (0.01) was used to generate adversarial examples with $\kappa = 10$. As can be seen in Table 1, the average L_∞ distortion under this configuration is 0.8. Therefore, adversarial examples were generated by PGD with $\epsilon = 0.8$. Clearly, performing elastic-net minimization aids in minimizing visual distortion. Furthermore, these results also emphasize the issues in solely using L_∞ to measure visual distortion.

5 Conclusion

The Madry Lab developed a defense model by focusing on training a sufficiently high-capacity network and using the strongest possible adversary. By their estimations, this adversary was PGD, which they motivate as the strongest attack utilizing the local first-order information about the network. Through extensive experiments, we demonstrate that EAD is able to outperform PGD in transferring in the targeted case. We also show that EAD is able to generate much less visually distorted transferable adversarial examples than PGD with comparable L_∞ distortion, due to the drastic reduction in L_1 and L_2 distortion. These results demonstrate the power of EAD, particularly in its transferability capabilities. Furthermore, these results indicate the drawbacks of using L_∞ as the sole distortion metric.

References

- [1] Liu, Y.; Chen, X.; Liu, C.; and Song, D. 2016. Delving into transferable adversarial examples and black-box attacks. *arXiv preprint arXiv:1611.02770*.
- [2] Tramèr, F.; Kurakin, A.; Papernot, N.; Boneh, D.; and McDaniel, P. 2017. Ensemble adversarial training: Attacks and defenses. *arXiv preprint arXiv:1705.07204*.
- [3] Chen, P.Y.; Sharma, Y.; Zhang, H.; Yi, J.; and Hsieh, C.J. 2017. EAD: Elastic-Net Attacks to Deep Neural Networks via Adversarial Examples *arXiv preprint arXiv:1709.04114*.
- [4] Madry, A.; Makelov, A.; Schmidt, L.; Tsipras, D.; and Vladu, A. 2017. Towards deep learning models resistant to adversarial attacks. *arXiv preprint arXiv:1706.06083*.
- [5] Szegedy, C.; Zaremba, W.; Sutskever, I.; Bruna, J.; Erhan, D.; Goodfellow, I.; and Fergus, R. 2013. Intriguing properties of neural networks. *arXiv preprint arXiv:1312.6199*.
- [6] Carlini, N., and Wagner, D. 2017b. Towards evaluating the robustness of neural networks. In *IEEE Symposium on Security and Privacy (SP)*, 39–57.
- [7] Goodfellow, I. J.; Shlens, J.; and Szegedy, C. 2015. Explaining and harnessing adversarial examples. *ICLR'15; arXiv preprint arXiv:1412.6572*.
- [8] Kurakin, A.; Goodfellow, I.; and Bengio, S. 2016b. Adversarial machine learning at scale. *ICLR'17; arXiv preprint arXiv:1611.01236*.

Table 2: Results of training the Madry Defense Model with a PGD adversary constrained under varying ϵ . ‘Nat Test Accuracy’ denotes accuracy on classifying original images. ‘Adv Test Accuracy’ denotes accuracy on classifying adversarial images generated by the same PGD adversary as was used for training.

Epsilon	Nat Test Accuracy	Adv Test Accuracy
0.1	99.38	95.53
0.2	99	92.65
0.3	98.16	91.14
0.4	11.35	11.35
0.5	11.35	11.35
0.6	11.35	11.35
0.7	10.28	10.28
0.8	11.35	11.35
0.9	11.35	11.35
1	11.35	11.35

6 Supplementary Material

6.1 Retraining the Madry Defense Model (Table 2)

The MNIST model released by the Madry Lab is adversarially trained using PGD with $\epsilon = 0.3$. Therefore, it is expected that the existing Madry Defense Model performs poorly against PGD attacks with $\epsilon > 0.3$.

In order to rectify this issue, the Madry Defense Model was trained with and evaluated against a PGD adversary with ϵ tuned from 0.1 to 1.0 under 0.1 increments. As suggested in [4], the PGD attack was run for 40 iterations, and to account for varying ϵ , the stepsize was set to $2\epsilon/40$.

The adversarial retraining results are shown in Table 2. These results suggest that the Madry Defense Model can not be successfully adversarially trained using a PGD adversary with $\epsilon > 0.3$. This is understandable as with such large ϵ , the visual distortion is clearly perceptible.

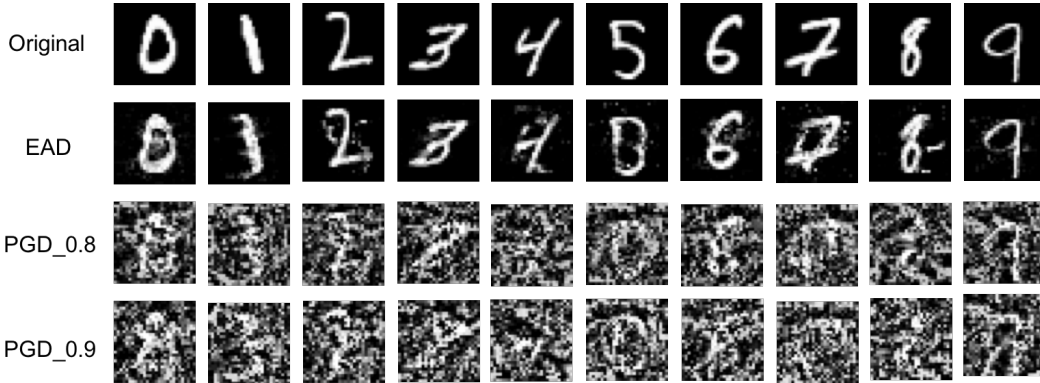


Figure 3: Visual illustration of adversarial examples crafted in the targeted case by EAD and PGD with similar average L_∞ distortion. As the adversarial examples generated by EAD have an average L_∞ distortion of 0.876, adversarial examples generated by PGD with $\epsilon = 0.8$ and $\epsilon = 0.9$ are shown.

6.2 Visual Comparison in the Targeted Case (Figure 3)

In Figure 3, adversarial examples generated by EAD are directly compared to those generated by PGD with similar average L_∞ distortion in the targeted case. EAD tuned to the optimal β (0.01) was used to generate adversarial examples with $\kappa = 10$. As can be seen in Table 1, the average L_∞ distortion under this configuration is 0.876. Therefore, adversarial examples were generated by PGD with $\epsilon = 0.8$ and $\epsilon = 0.9$. It can be seen that further distortion is needed to generate transferable

Table 3: Comparison of tuned PGD, I-FGM, C&W, and EAD adversarial examples at various confidence levels generated from attacking a single model. ASR means attack success rate (%). The distortion metrics are averaged over successful examples.

Attack Method	Confidence	Targeted				Non-Targeted			
		ASR	L_1	L_2	L_∞	ASR	L_1	L_2	L_∞
PGD	None	41.2	214.5	10.18	0.7	99.7	237.1	11.52	0.7
I-FGM	None	39.2	133.6	6.801	0.87	99.3	160.8	8.395	0.7
C&W	10	0.1	17.4	1.112	0.19	1.8	12.57	0.801	0.156
	30	4.8	47.9	3.235	0.69	8.5	35.5	2.371	0.53
	50	51.5	81.67	5.455	0.913	46.9	59.18	3.873	0.765
	70	75.8	114.6	7.499	0.986	89.7	82.85	5.375	0.925
EAD	10	3.6	13.21	2.22	0.848	11.8	10.91	1.856	0.725
	30	32.7	33.75	3.735	0.963	44.9	25.98	3.129	0.906
	50	67.2	59.05	5.404	0.998	81	41.89	4.319	0.978
	70	82.7	91.15	7.227	1	94.7	61.69	5.572	0.997

adversarial examples in the targeted case, however, the benefit that elastic-net minimization applies for improving visual quality is still clearly evident.

6.3 Single Model Results (Table 3)

When using a single model for generating transferable adversarial examples, the highest attack success rate (ASR) for EAD in both the targeted and non-targeted cases was, again, yielded at $\beta = 0.01$. Regarding ϵ , in the targeted case, the highest ASR was yielded at $\epsilon = 0.7$ and $\epsilon = 1$ for PGD and I-FGM, respectively. In the non-targeted case, the lowest ϵ at which the highest ASR was yielded was at $\epsilon = 0.7$ for both PGD and I-FGM.

In Table 3, the results of tuning κ for C&W and EAD at $\beta = 0.01$ are provided, and are presented with the results for PGD and I-FGM at the aforementioned ϵ values for comparison. Alike the results when using an ensemble of models, in the targeted case, EAD outperforms C&W at all κ , and at $\kappa \geq 50$, EAD’s adversarial examples unexpectedly have lower average L_2 distortion. Both EAD and C&W at properly tuned κ outperform PGD and I-FGM with much lower L_1 and L_2 distortion.

In the non-targeted case, it is observed that, alike the ensemble results, EAD outperforms C&W at all κ . Yet here, PGD and I-FGM outperform EAD in terms of ASR. However, as the adversarial examples generated by PGD and I-FGM have such large L_1 and L_2 distortion, one can expect the perturbations to be visually perceptible.

6.4 Beta Search for EAD (Tables 4 and 5)

In Table 4, the results of tuning β when generating adversarial examples with EAD attacking an ensemble of models are presented. In Table 5, the results of tuning β when generating adversarial examples with EAD attacking a single model are presented. In both cases, but more so in the ensemble case, one can see at the optimal κ in terms of ASR, tuning β plays relatively little effect in improving the ASR. However, at lower κ , which is applicable when visual quality is important, increasing β plays a rather significant role in improving the ASR. This indicates that for generating transferable adversarial examples with minimal visual distortion, minimizing the L_1 distortion is more important than minimizing L_2 , or, by extension, L_∞ .

6.5 Epsilon Search for PGD and I-FGM (Figures 4 and 5)

In Figure 4, the results of tuning ϵ when generating adversarial examples with PGD and I-FGM attacking an ensemble of models are shown. In Figure 5, the results of tuning ϵ when generating adversarial examples with PGD and I-FGM attacking a single model are shown. The results simply show that by adding large amounts of visual distortion to the original image, an attacker can cause a target defense model to misclassify. However, when compared to EAD, the adversarial examples of PGD and I-FGM are less transferable and more visually perceptible, as indicated by the drastic increase in their L_1 and L_2 distortion.

Table 4: Analysis of adversarial examples generated by EAD tuned with various beta values and confidence levels when attacking an ensemble of models. ASR means attack success rate (%). The distortion metrics are averaged over successful examples.

Beta	Confidence	Targeted				Non-Targeted			
		ASR	L_1	L_2	L_∞	ASR	L_1	L_2	L_∞
1e-4	10	1.4	31.67	2.435	0.614	5.7	23.52	1.795	0.487
	30	67.5	64.84	4.526	0.894	71	50.58	3.641	0.812
	50	98.7	107.3	7.094	0.997	98.9	76.68	5.361	0.965
	70	74.3	163.6	9.993	1	99.8	112.9	7.466	0.998
1e-3	10	4.8	26.31	2.489	0.701	14.1	20.71	2.087	0.622
	30	75.5	59.62	4.642	0.941	83.5	43.16	3.69	0.871
	50	98.6	99.98	7.185	0.999	99.3	69.56	5.411	0.979
	70	73	155.2	10	1	99.8	106.4	7.526	0.999
1e-2	10	27.4	25.79	3.209	0.876	39.9	19.19	2.636	0.8
	30	85.8	49.64	5.179	0.995	94.5	34.28	4.192	0.971
	50	98.5	93.46	7.711	1	99.6	57.68	5.839	0.999
	70	67.2	148.9	10.36	1	99.8	90.84	7.719	1

Table 5: Analysis of adversarial examples generated by EAD tuned with various beta values and confidence levels when attacking a single model. ASR means attack success rate (%). The distortion metrics are averaged over successful examples.

Beta	Confidence	Targeted				Non-Targeted			
		ASR	L_1	L_2	L_∞	ASR	L_1	L_2	L_∞
1e-4	10	0.1	16.03	1.102	0.186	2	12.68	0.867	0.193
	30	2.8	43.02	2.88	0.658	9.8	34.21	2.33	0.558
	50	36.8	75.5	4.76	0.891	41.8	58.06	3.723	0.773
	70	75.1	107.7	6.629	0.988	84.6	81.18	5.063	0.924
1e-3	10	0.3	16.23	1.45	0.379	2.5	11.79	1.037	0.286
	30	7.5	39.42	3.025	0.739	15.4	30.13	2.453	0.658
	50	49.8	69.66	4.892	0.942	53.3	52.67	3.779	0.839
	70	78	99.68	6.711	0.996	88	74.47	5.096	0.951
1e-2	10	3.6	13.21	2.22	0.848	11.8	10.91	1.856	0.725
	30	32.7	33.75	3.735	0.963	44.9	25.98	3.129	0.906
	50	67.2	59.05	5.404	0.998	81	41.89	4.319	0.978
	70	82.7	91.15	7.227	1	94.7	61.69	5.572	0.997

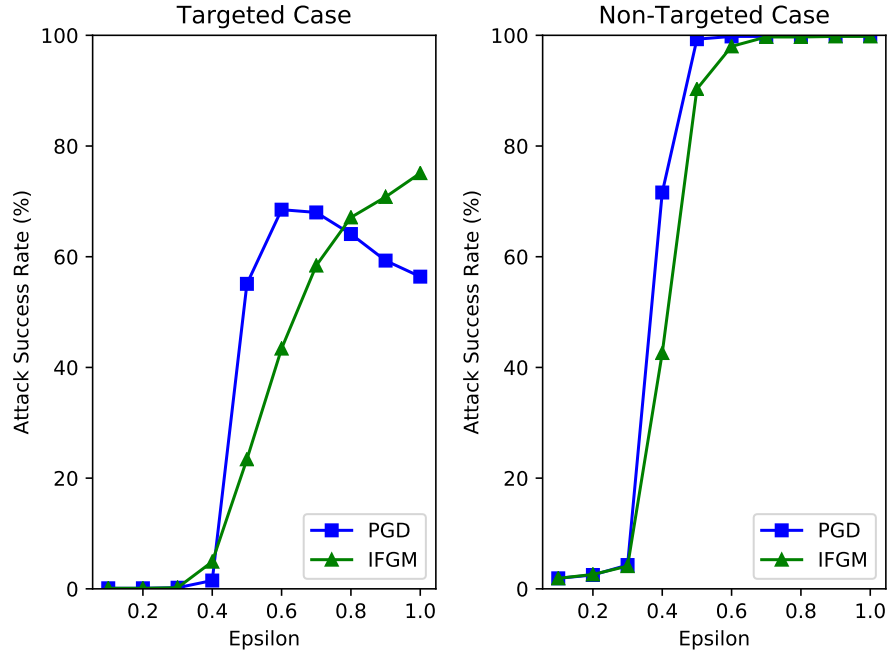


Figure 4: Attack transferability of adversarial examples generated by PGD and I-FGM with various ϵ values when attacking an ensemble of models.

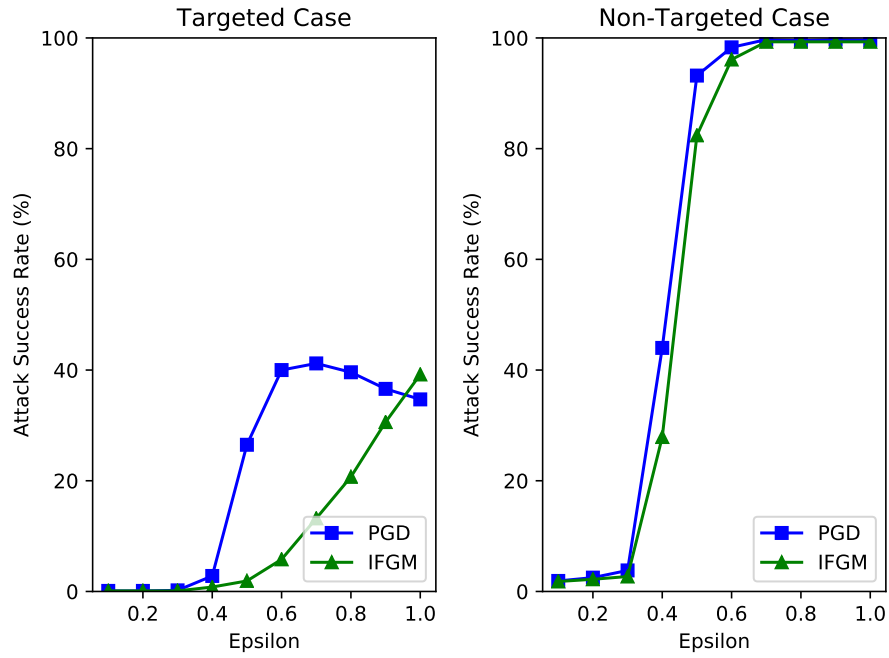


Figure 5: Attack transferability of adversarial examples generated by PGD and I-FGM with various ϵ values when attacking a single model.